33rd Annual International Conference of the IEEE EMBS
Boston, Massachusetts USA, August 30 - September 3, 2011

An Algorithm for Source Signal Extraction from the Peripheral Nerve

Yuang Tang, Brian Wodlinger and Dominique M. Durand *Fellow, IEEE*

***Abstract*—Extracting physiological signals to control external devices such as prosthetics is a field of research that offers great hope for patients suffering from disabilities. In this paper, a novel source signal extraction algorithm, based on the source localization method *Champagne*, is presented. The algorithm constructs spatial filters that not only maximizes the signal to noise ratio (SNR > 13dB) of the source activities but also minimizes the cross-talk interference between the sources $10log(\frac{P(source\ of\ interest)}{P(interference\ sources)}) > 14\ dB$.**

I. Introduction

Research into the extraction of physiological source signals from human subjects to control external devices offers numerous possibilities to improve the lives of disabled patients. In this paper, we propose an algorithm for extracting source signals from the peripheral nerve recorded with Flat Interface Nerve Electrodes (FINE). Recordings from the peripheral nerve offer several advantages over brain signals: (a) the functional anatomy of the peripheral nerves are known and is considerably more structured and simpler. This can lead to less interferences and more stable source signals. (b) The physiological functions of the individual nerves are clearly understood, which facilitates the generation of controlled signals by human subjects. (c) The procedures are less invasive compared to ECoG and intracranial electrode placement surgeries but can acquire better source signals compared to surface EEG.

Our proposed algorithm is based on the Bayesian techniques described in [1, 2] called *Champagne*. The algorithm utilizes a novel strategy to construct spatial filters that not only maximize the SNR of the individual source signals but also minimize the cross-talk between the source signals. This is a crucial aspect of source signal extraction for control since cross-talk amongst sources are just as debilitating as noises in the system. In the following sections, we will first detail the acute *in-vivo* experimental setup used to generate the biological source signals, then the details of the proposed algorithm is given and finally the algorithm is implemented and evaluated with physiological signals.

Manuscript received March 27th, 2010. This work was supported in part by the NIH-NINDS-ARRA-Supplement Grant: 3R01NS032845-14S1.

Y. Tang is with the Department of Biomedical Engineering, Case Western Reserve University, Cleveland, OH 44106 USA (phone:405-503-9920; fax: 216-368-4872; e-mail: dyt1@ case.edu).

B. Wodlinger was with the Department of Biomedical Engineering, Case Western Reserve University, Cleveland, OH 44106 USA. He is now with the Department of Physical Medicine and Rehabilitation, University of Pittsburgh, Pittsburgh, PA 15260 USA (e-mail: bcw12@case.edu).

D.M. Durand is with the Department of Biomedical Engineering, Case Western Reserve University, Cleveland, OH 44106 USA (email: dxd6@ case.edu).

II. Methods

If we record a segment of nerve activity Y, with the number of time points length N, from $K = 16$ electrode contacts ($Y \in \mathbb{R}^{KxN}$), then it is the objective of this project to find a set of spatial filters $F_j \in \mathbb{R}^K$ that can extract the individual source signals X_j from the recorded signals Y i.e.

$$X_j = F_j Y, j = 1{:}\, D_X \quad (1)$$

D_X is the number of independent sources.

A. Data Collection

In this section we detail the methods for the acquisition of Y. New Zealand White Rabbits are anesthetized with 20-50 mg/kg IM ketamine and 5 mg/kg IV diazepam and maintained with 60 mg/kg IV alpha-chloralose (followed by one quarter dose every 2 hours or as needed) and .02 mg/kg IM buprenex. All protocols are approved by the Case Western Reserve University IACUC. Recordings are made from a novel 16-channel tripolar FINE placed on the sciatic trunk near the popliteal fossa. The Fine offers better recording selectivity by reshaping the geometry of the nerve [3, 4]. The signals are AC coupled, amplified, multiplexed and low-pass filtered at 5 kHz by an RHA1016 preamplifier chip (Intan Technologies, Utah). A National Intruments data acquisition card is used to perform A-to-D conversion and sampling at 15 kHz/channel. Tripolar stimulating FINEs are placed on the Tibial and Peroneal branches of the Sciatic nerve, distal to the recording cuff. 130Hz sinusoidal electrical stimulations are separately applied to each individual nerve branch to simulate source activities, so D_X = 2. Sinusoids are used for easy artifact removal. Recorded signals are post-processed using an 800Hz – 3 kHz band-pass filter in order to reduce any non-essential EMG and stimulation artifacts. The resultant evoked nerve activities are then used as inputs into the proposed algorithm where spatial filters are constructed for each source (Peroneal|Tibial).

B. Spatial Filter Construction

Based on *Champagne*, the problem of extracting the individual source activities from the measured sciatic nerve signals Y, can be modeled as

$$Y = LS + e \quad (2)$$

where $S \in \mathbb{R}^{MxN}$ are the N time point activities of the M pixels within the cross section of the FINE finite element model. Each pixel can be seen as a potential source that have influences on the K FINE contacts described by the lead field matrix $L \in \mathbb{R}^{KxM}$. The various noise and interferences that exist within the system are described by e. Detailed explanation of the lead field matrix L can be found in [5]. In short, a rectangular finite element model of the FINE positioned over an empty epineurium enclosing a homogeneous volume conductor is created, Fig. 1a.

a

b

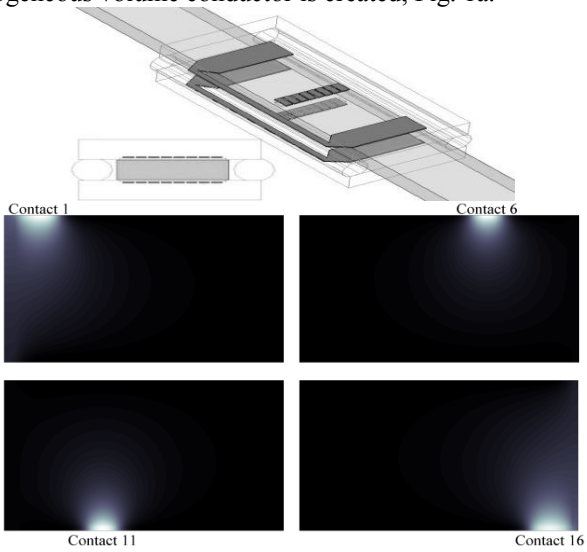

Fig 1. (a) The finite element model of the FINE electrode measuring 5mm by 1.5mm and divided into 208 by 82 pixels [5]. (b) The pixel-sensitivity described by the lead field matrix L for electrodes 1, 6, 11 and 16.

The FINE, measuring 5mm by 1.5mm, consists of 16 contacts with contacts 1 to 8 arranged from top left to top right and contacts 9 to 16 from bottom left to bottom right. The cross section of the FINE is divided into 208 by 82 pixels, which leads to M = 17056. In Fig. 1b, the sensitivities of the four contacts (1, 5, 11 and 16) to the M pixels are plotted.

To estimate the source locations we first introduce the following likelihood model based on (2)

$$p(Y|S) \propto exp\left(-\frac{1}{2}\|Y - LS\|^2_{C_e}\right) \tag{3}$$

where $\|Q\|_C = \sqrt{trace[Q^T C^{-1} Q]}$. C_e is an unknown noise covariance matrix that is estimated later. The sources S are modeled as independent zero mean Gaussian distributions with covariance C_{S_i} for S_i

$$p(S_i^n) = \mathcal{N}(S_i^n|\, 0, C_{S_i}) \tag{4}$$

where $n = 1{:}N$. We also make the assumption that the sources are independent in time, leading to the source prior

$$p(S|C_S) \propto exp\left(-\frac{1}{2} trace[S^T C_S^{-1} S]\right) \tag{5}$$

C_S is a diagonal matrix with the covariance C_{S_i} for each pixel $S_i\ (i = 1{:}M)$ located along the diagonal. The approximation of C_S infers the pixel locations where the sources most likely reside. When this approximation is complete, spatial filters F_j for each of the two sources $S_j = F_j Y, F_j \in \mathbb{R}^K$ can be constructed by utilizing the expectation of S

$$\begin{aligned} E_{p(S|Y,C_S)} &= C_S L^T (C_e + L C_S L^T)^{-1} Y \\ F_j &= C_{S,j} L^T (C_e + L C_{S,j} L^T)^{-1} \end{aligned} \tag{6}$$

here j points to the two sources Peroneal|Tibial, and $C_{S,j}$ is the pixel covariance matrix obtained for each source. The learned solution of C_S should maximize

$$p(Y|C_S) = \int p(Y|S) p(S|C_S) dS \tag{7}$$

which reduces to the minimization of the cost function

$$\begin{aligned} L(C_s) &= trace[C_Y C_E^{-1}] + \log(|C_E|) \\ C_E &= C_e + L C_S L^T \text{ and } C_Y = d_t^{-1} Y Y^T \end{aligned} \tag{8}$$

This cost function balances the differences between the learned covariance model C_E and the empirical data covariance C_Y through the term $trace[C_Y C_E^{-1}]$ against the complexity of the solution $\log(|C_E|)$. Pixels that are not learned sources have C_S values approaching zero. Details of the update rules for iterating to a C_S solution can be found in [2].

The last piece of the puzzle left is the approximation of C_e. The procedure for the determination of C_e is described in [1]. Briefly, the nerve recordings Y are modeled as a combination of source signals X, interference signals U and random noise V.

$$Y = AX + BU + V \tag{9}$$

The source and interference signals are assumed to be independent Gaussian distributions with zero mean and unit precision. The random noise term V is described by a diagonal precision matrix C_V. Given an initial choice of the number of sources and interferences to be learned, the algorithm utilizes variational Bayes expectation maximization to learn the set of model parameters that best fit the data covariance matrix C_Y by

$$C_Y \approx AA^T + BB^T + C_V^{-1} \tag{10}$$

where the learned interference and noise parameters are used to compute C_e.

$$C_e = BB^T + C_V^{-1} \tag{11}$$

With the approximation of C_e complete, C_S can be learned and spatial filters constructed for each source. While the spatial filters constructed this way maximize the SNR for each source, they do not take into account the cross-talk between the sources. To minimize cross-talk, we propose a novel strategy. For each source $X_i, i = 1{:}D_X$, instead of (11), we use the definition below to compute the corresponding noise|interference parameter $C_{i,e}$ as

$$C_{i,e} = B_i B_i^T + C_{i,V}^{-1} + \sum_{j=1, j\neq i}^{D_x} A_j A_j^T \quad (12)$$

By incorporating this additional term into the definition of C_e, the algorithm effectively treats sources, that are not the target of the current spatial filter, as interferences. This modification leads to spatial filter solutions that both maximize SNR and minimize cross-talk.

C. Implementation

The proposed algorithm requires an initial selection of the number of source and interference signals to be approximated in (9). However the models for sources and interferences are identical and not easily distinguished. This is because the algorithm is originally designed to take advantage of a pre-stimulus period, when the sources are silent and only interferences and random noises exist. The pre-stimulus data is used to learn the model parameters $B, U \text{ and } V$. These parameters are then held constant while $A \text{ and } X$ are learned with the post-stimulus data. In this study, the CAP like activities evoked via the 130 Hz sinusoidal stimulation have high signal strength compared to background activities. As such, we can use (13) instead of (9) to approximate both the source and interference signals together knowing that the source components should have $\|E_j\|, j = 1{:}J$ that are significantly higher compared to background activities. J is the combined number of sources and interferences.

$$\begin{aligned} &Y = EZ + V \\ &E = (A\ B), Z = \begin{pmatrix} X \\ U \end{pmatrix} \\ &E \in \mathbb{R}^{KxJ}, Z \in \mathbb{R}^{JxN} \end{aligned} \quad (13)$$

In this study J is set to 15. The learned $\|E_j\|$ are ranked in descending order. The learned factor, associated with $\|E_1\|$, along with other factors that satisfy $\|E_j\| > 0.25\|E_1\|$ are considered to be part of the source signal while the remaining factors are considered interferences. In the remaining section, the proposed algorithm is evaluated with data acquired from 6 rabbits, with each rabbit providing two sets of trials (left and right hind legs).

III. RESULTS

During experimentation, 30 seconds stimulation epochs are administered separately to the Tibial and Peroneal nerve branches. The CAP like responses evoked by the stimulation paradigm for both nerve branches are shown in Fig. 2. In the figure, 0.1s of recorded and preprocessed nerve activities averaged across the 16 FINE contacts are plotted.

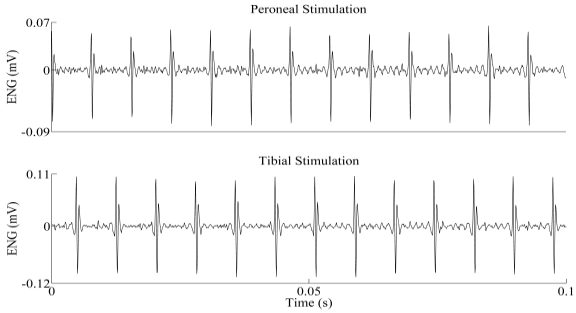

Fig 2. 0.1s of evoked Peroneal and Tibial signals averaged across the 16 FINE contacts.

Each 30s data segment is split into two 3s and 27s segments where the 3s segments are used to learn the spatial filters and the 27s segments are used to evaluate their performance. The spatial filters are judged by the SNR of the extracted source signals and the amount of cross-talk between the sources. Since we know the time of the evoked CAP responses, for each source j, we can average all its CAP responses together to form Y_j^{CAP} that contains mainly source activities.

$$X_j^{CAP}(n) = \frac{1}{K_{stim}} \sum_{k=1}^{K_{stim}} X_j(T_k + n), n = 0{:}W-1 \quad (14)$$

K_{stim} is the set number of evoked responses to be averaged, T_k is the start point of the kth evoked response and W=23 is the width of the CAP responses in sampling points. Let $X_j^{'}$ be all the sample points of $X_j$that are not within a CAP response, then the SNR of the extracted source X_j can be defined as

$$SNR(X_j) = 10\log\left(\frac{P(X_j^{CAP})}{P(X_j^{'})}\right) \quad (15)$$

where P is power. To measure cross-talk between two sources for a given filter F_j we measure the cross-talk ratio (CTR) as

$$CTR(F_j) = 10\log\left(\frac{P(X_j^{CAP})}{P(X_{i\neq j}^{CAP})}\right) \quad (16)$$

Spatial filters are constructed over 3s data segments using both the traditional *Champagne* algorithm i.e. (11) and the proposed algorithm (12). To illustrate the improvement in cross-talk suppression using the proposed algorithm, we build a test data segment by concatenating Peroneal and Tibial evoked signals, with its average signal across the 16

FINE contacts shown at the top of Fig. 3. In the figure, the Peroneal and Tibial activities are delineated by arrows. Spatial filters (PFilter, TFilter) constructed using the proposed algorithm as well as the traditional *Champagne* (ChampP, ChampT) for the extraction of Peroneal and Tibial signals respectively are applied to the test signal and the results plotted.

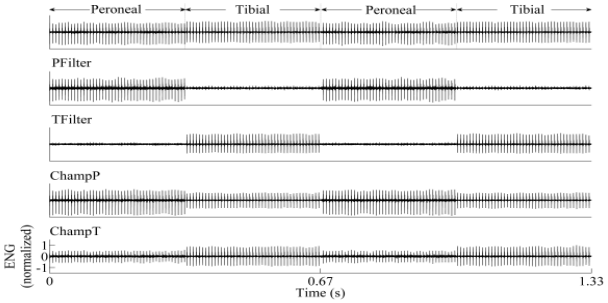

Fig 3. The test signal consisting of both Peroneal and Tibial activities are shown in the top plot. The filtered outputs by the PFilter, TFilter, ChampP and ChampT are illustrated in subsequent plots.

It can be observed that while ChampP and ChampT both extracted their signals of interest, there is considerable cross-talk i.e. Tibial activities are significant in the ChampP filtered signals while Peroneal activities are evident in the ChampT filtered signals. These cross-talks greatly limit the utility of the control sources because they are effectively interferences that limit the dynamic range of the control signals. In comparison, PFilter and TFilter do a much better job of suppressing cross-talk between the sources. In both filtered signals, there is little activity from the interfering source, achieving both high SNR and CTR. A comparison of the filters' sensitivity fields are shown in Fig. 4.

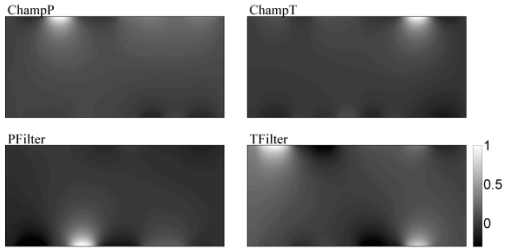

Fig 4. Illustration of each filter's sensitivity to the M pixels. The brighter areas indicate the incorporation of those pixel activities while the darkest areas represent subtractions.

The original filters ChampP and ChampT combine activities from pixels that are often under the influence of the interfering source, resulting in substantial cross-talk. Filters PFilter and TFilter not only avoid pixels that are heavily impacted by the interfering source but they often subtract the activities of those pixels from the extracted source signal of interest. Fig. 5 plots the average performances, over 12 trials, of the proposed algorithm and *Champagne*, against the input signals' SNR and CTR. Since the exact input signals are not known we approximate them with the average signals across the 16 FINE contacts. These approximated inputs have mean SNR > 15dB but poor CTR < 0.4dB across the Peroneal and Tibial nerves. Compared to the input, the *Champagne* filters are able to achieve similar mean SNR performance > 15dB for both Peroneal and Tibial signals and higher mean CTR > 1.9dB. However, these CTR values

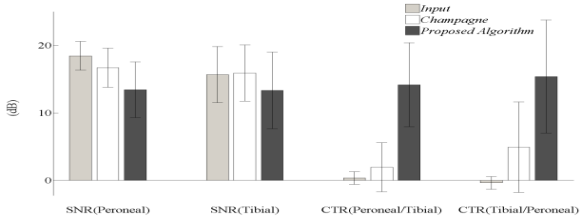

Fig 5. Performance comparisons between *Champagne* and the proposed algorithm.

are still low and limit the utility of the extracted signals despite the higher SNRs. Filters constructed using the proposed algorithm exhibits considerable improvement in cross-talk suppression, average CTR > 14dB while maintaining average SNR > 13dB. This is a significant improvement in that the extracted signals are no longer constrained by the poor CTR values. The reduced SNR performance is expected for these filters since their solution spaces are limited by cross-talk interferences.

IV. Conclusion

In this paper, we proposed a novel source signal extraction method based on the Bayesian algorithm *Champagne*. The algorithm demonstrated its ability to balance both the SNR of the extracted source signals and the amount of cross-talk between the signals. While effective, the proposed method requires the ability to evoke individual sources separately. We are currently developing an improvement by utilizing an iterative independent component analysis algorithm to extract source signals that are mixed in time. Eventually we hope to implement the algorithm to acquire voluntary signals from human amputee patients for the control of artificial limbs.

Acknowledgment

Y.T. author thanks Dr. Sri Nagarajan for his help with *Champagne*.

References

[1] Nagarajan, S.S., et al., *A probabilistic algorithm for robust interference suppression in bioelectromagnetic sensor data.* Statistics in medicine, 2007. **26**(21): p. 3886-910.

[2] Wipf, D.P., et al., *Robust Bayesian estimation of the location, orientation, and time course of multiple correlated neural sources using MEG.* NeuroImage, 2010. **49**(1): p. 641-55.

[3] Durand, D.M., P. Yoo, and Z. Lertmanorat. *Neural interfacing with the peripheral nervous system*. in *Engineering in Medicine and Biology Society, 2004. IEMBS '04. 26th Annual International Conference of the IEEE*. 2004.

[4] Yoo, P.B. and D.M. Durand. *The recording properties of a multi-contact nerve electrode as predicted by a finite element model of the canine hypoglossal nerve*. in *Engineering in Medicine and Biology Society, 2004. IEMBS '04. 26th Annual International Conference of the IEEE*. 2004.

[5] Wodlinger, B. and D.M. Durand, *Localization and Recovery of Peripheral Neural Sources With Beamforming Algorithms.* Neural Systems and Rehabilitation Engineering, IEEE Transactions on, 2009. **17**(5): p. 461-468.